

One-loop corrections to the E-type α -attractor models of inflation and primordial black hole production

Daniel Frolovsky ^{a,*} and Sergei V. Ketov ^{a,b,c,#}

^a Department of Physics and Interdisciplinary Research Laboratory,
Tomsk State University, Tomsk 634050, Russian Federation

^b Department of Physics, Tokyo Metropolitan University, Tokyo 192-0397, Japan

^c Kavli Institute for the Physics and Mathematics of the Universe (WPI),
The University of Tokyo Institutes for Advanced Study, Chiba 277-8583, Japan

* frolovsky@mail.tsu.ru, # ketov@tmu.ac.jp

Abstract

The one-loop corrections (1LC) to the power spectrum of scalar perturbations, arising from cubic interactions in the single-field E-type α -attractor models of inflation and primordial black hole (PBH) production, are numerically calculated. The results demonstrate the 1LC contributes merely a few percent to the tree-level power spectrum. The model parameters are chosen to predict the PBH masses in the asteroid-mass range, while maintaining consistency with the cosmic microwave background (CMB) observations within 1σ confidence levels, and obeying the upper limits on μ -distortions. The PBH formed on scales smaller than the inflation scale can constitute a significant fraction of the present dark matter (DM). The PBH-induced gravitational waves (GW) may be detectable by the future space-based gravitational interferometers. We also consider a reconstruction of the scalar potential from possible GW observations and present a numerical approach tested in the parameter space of the model.

1 Introduction

Cosmic microwave background (CMB) measurements [1] provide valuable insights into the early universe but do not uniquely fix the underlying model of inflation. Though the simplest single-field slow-roll (SR) models of inflation are tightly constrained by the CMB measurements and the Swampland Conjectures [2] about their Ultra-Violet (UV) completion in quantum gravity, significant uncertainties remain. Those uncertainties leave room for constructing more general models that not only describe inflation but also formation of primordial black holes (PBH) from gravitational collapse of large scalar perturbations [3, 4].

The standard mechanism of PBH production in single-field models of inflation is via engineering a near-inflection point in an inflaton potential on energy scales under the scale of inflation, which cannot be probed by CMB [5]. Inflaton dynamics is driven by the inflaton potential, whereas adding PBH production generically leads to lower values of the CMB scalar tilt n_s , often in tension with CMB measurements. To get viable inflation with PBH production, and avoid tension with the CMB observations, fine-tuning of the inflaton potential parameters is needed. However, then another problem arises because the classical fine-tuning may be destroyed by quantum loop corrections, as was first observed in Ref. [6]. The enhancement of the power spectrum of scalar perturbations, related to large perturbations and required for efficient PBH production beyond the Hawking evaporation limit, has to be 6 or 7 orders of the magnitude higher against the CMB spectrum, which may imply large quantum corrections. Demanding a suppression of the loop corrections against the tree-level contribution can be used for an even tighter discrimination between the models of inflation with related PBH production.

The first version of Ref. [6], which attracted considerable attention in the literature (see e.g., the references in Ref. [6]), claimed that *any* single-field model of inflation with PBH production suffers from a large one-loop correction that destroys the viability of those models against the CMB observations, at least in the case of sharp transitions from slow-roll (SR) to ultra-slow-roll (USR) regimes. This conclusion was later criticized on the ground that physics on higher scales usually decouples from lower-scale physics, so that, in particular, PBH production could not significantly influence inflation [7]. After that many papers [8–17] on the same subject led to a conclusion that the quantum loop corrections are model-dependent and, therefore, should be calculated on the case-by-case basis.

An important class of viable single-field models of inflation is given by the α -attractors [18, 19]. Those models are extensions of the Starobinsky model of inflation [20], which is recovered at $\alpha = 1$, though with a more general (α -dependent) prediction for the CMB tensor-to-scalar ratio r . The basic α -attractor models are divided into two types depending upon the global shape of the inflaton scalar potential,

$$\text{E-type: } V \sim \left(1 - e^{-\sqrt{\frac{2}{3\alpha}} \phi/M_{\text{Pl}}}\right)^2, \quad \text{and} \quad \text{T-type: } V \sim \tanh^2 \frac{\phi/M_{\text{Pl}}}{\sqrt{6\alpha}}, \quad (1)$$

as a function of canonical inflaton ϕ . Both the E-type and T-type α -attractor models can be generalized further, without changing their predictions for inflation, by using proper functions $f(y)$ and $g(\tilde{r})$, respectively, with the potentials

$$\text{E-type: } V \sim f^2(y), \quad \text{and} \quad \text{T-type: } V \sim g^2(\tilde{r}), \quad (2)$$

where the variables y and \tilde{r} are defined as

$$y = \exp\left(-\sqrt{\frac{2}{3\alpha}} \phi/M_{\text{Pl}}\right), \quad \tilde{r} = \tanh\left(\frac{\phi/M_{\text{Pl}}}{\sqrt{6\alpha}}\right). \quad (3)$$

It is worth mentioning that the full-square-form of the potentials in Eq. (2) allows their embedding into supergravity [21].

After expanding the functions $f(y)$ and $g(\tilde{r})$ in power series and keeping a few leading terms, one may engineer a large peak in the power spectrum of scalar perturbations, leading to PBH production. In the case of the generalized T-models, this construction was first used in Ref. [22], where a quintessence model was proposed with the inflaton potential

$$V = V_0 [c_0 + c_1\tilde{r} + c_2\tilde{r}^2 + c_3\tilde{r}^3]^2 . \quad (4)$$

Here, the constant $V_0 > 0$ is related to the amplitude of scalar perturbations, and the parameters c_0, c_1, c_2 , and c_3 are all dimensionless. Fine-tuning of the parameters allows PBH production [22], though at the price of low tilts n_s , while more precise (later) CMB measurements ruled out the model (4) before examining loop corrections.

Therefore, it makes sense to turn to the generalized E-models with PBH production. To get a good (within 1 sigma) agreement with the latest CMB measurements, it was proposed in Refs. [23, 24] to consider the E-model with the potential

$$V(\phi) = \frac{3}{4}M^2M_{\text{Pl}}^2 [1 - y - \theta y^{-2} + y^2(\beta - \gamma y)]^2 , \quad (5)$$

where M is the inflaton mass, and β, γ, θ are the additional dimensionless parameters. In particular, it was found [23] that demanding a regular function $f(y)$ at the origin $y = 0$ does not allow agreement with the Planck-measured value of n_s within 1 sigma in the cases, where $f(y)$ facilitates PBH production across a wide mass range. However, adding a negative power of y resolves this tension [24]. In contrast to the T-models (4), where adding the negative powers of \tilde{r} would imply a singularity at $\phi = 0$, the E-models (5) have the infinite potential at $y = 0$ and $y = +\infty$ that correspond to $\phi = +\infty$ and $\phi = -\infty$, respectively.

To further investigate the validity of the generalized E-models for inflation and PBH production, one has to evaluate an impact of the loop corrections in the case of (5) because the amplified fluctuations associated with PBH production may lead to the loop corrections exceeding the tree-level contribution calculated by using the linear perturbation equations in Refs. [23, 24]. Should those loop corrections be too large, it would indicate a breakdown of perturbativity in the model, thus challenging the reliability of its predictions for the CMB observables. This issue has been the subject of intensive research in the recent literature [6–17]. In this paper, we numerically compute the one-loop correction (1LC) to the scalar power spectrum in the generalized E-type α -attractor model (5) by following the approach proposed in Ref. [25].

The paper is organized as follows. In Sec. 2 we reparameterize the model (5) in terms of the new parameters directly related to the shape of the inflaton potential and explore the potential for various values of the parameter α . The perturbative dynamics of inflaton during SR and USR is numerically evaluated in Sec. 3. The one-loop (1LC) correction is computed in Sec. 4. The PBH-production-induced gravitational waves (GW) are derived in Sec. 5, in the second order with respect to perturbations. The inverse procedure from the given GW spectrum back to the power spectrum and a subsequent reconstruction of the inflaton potential are outlined in Sec. 6, where this procedure is applied to our E-model. In Sec. 7 we summarize our main results. Sec. 8 is our conclusion.

2 The Model

The standard (quintessence) action of single-field inflation models reads

$$\mathcal{S} = \int d^4x \sqrt{-g} \left(\frac{1}{2}R - \frac{1}{2}(\partial_\mu\phi)^2 - V(\phi) \right), \quad c = \hbar = M_{\text{Pl}} = 1, \quad (6)$$

where ϕ is a canonical inflaton field, and $V(\phi)$ represents its potential.¹

The scalar potential of the E-type α -attractor model (5) can be rewritten in terms of the new dimensionless parameters ϕ_i and σ defined by

$$\beta = \frac{\exp\left(\sqrt{\frac{2}{3\alpha}}\phi_i\right)}{1 - \sigma^2}, \quad \text{and} \quad \gamma = \frac{\exp\left(2\sqrt{\frac{2}{3\alpha}}\phi_i\right)}{3(1 - \sigma^2)}, \quad (7)$$

that have the simple geometrical meaning: at $\sigma = 0$ the potential has an inflection point at $\phi = \phi_i$, and when $0 < \sigma \ll 1$, the potential has a local minimum y_{ext}^- to the right of the inflection point and a local maximum y_{ext}^+ to the left of the inflection point. Both extrema are symmetrically located around the inflection point as

$$y_{\text{ext}}^\pm = y_i (1 \pm \sigma). \quad (8)$$

The parameter θ governs the slope of the plateau in the potential on CMB scales, allowing us to achieve precise tuning of the scalar tilt n_s , and the tensor-to-scalar ratio r [24]. The potential (5) realizes the double inflation scenario with an USR phase between two SR regimes of inflation, leading to a large enhancement of the power spectrum of scalar perturbations and, thus, the PBH production. The profiles of the scalar potential for various values of the α -parameter are given in Fig. 1.

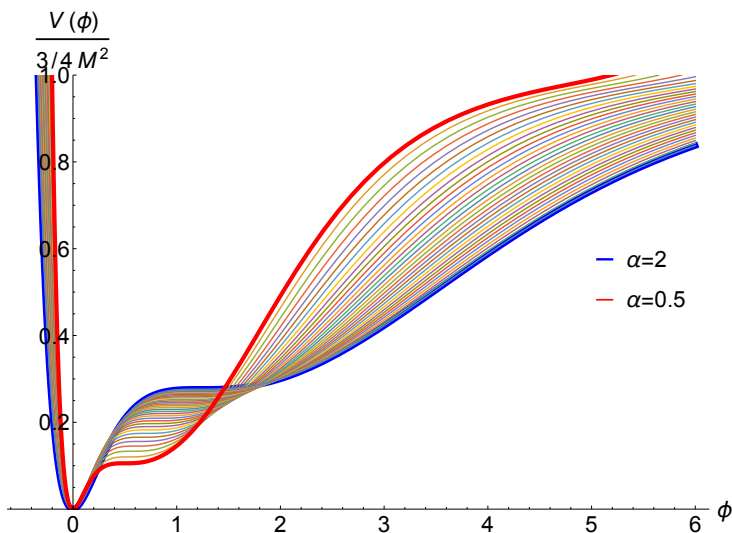


Figure 1: The profiles of the scalar potential in the E-model for $\alpha \in [0.5, \dots, 2]$. The scalar potential (5) is shifted to get $V(0) = 0$ for all α . The other parameters of the model are given by set 1 of Table 1 in Section 7.

3 Background evolution and curvature perturbations

The evolution of inflaton field in a (flat) Friedmann-Lemaitre-Robertson-Walker (FLRW) universe is described by the standard (Klein-Gordon and Friedmann) equations:

$$\ddot{\phi} + 3H\dot{\phi} + V_{,\phi} = 0, \quad 3H^2 = \frac{1}{2}\dot{\phi}^2 + V(\phi), \quad \dot{H} = -\frac{1}{2}\dot{\phi}^2, \quad (9)$$

where $H(t) \equiv \dot{a}/a$ is Hubble function, $a(t)$ is the cosmic scale factor in the (flat) FLRW metric, $ds^2 = -dt^2 + a^2(dx_1^2 + dx_2^2 + dx_3^2)$, $V_{,\phi} = dV/d\phi$, and the dots denote the time

¹We use the mostly-plus signature of spacetime and the standard notation of General Relativity.

derivatives. It is more convenient to use e-folds instead of time, which are defined by

$$N = \int H(t) dt . \quad (10)$$

Then, the equations of motion read

$$H^2 \phi'' + HH' \phi' + 3H^2 \phi' + V_{,\phi} = 0, \quad H^2 = \frac{2V(\phi)}{6 - (\phi')^2}, \quad H' = -\frac{1}{2}(\phi')^2 H, \quad (11)$$

or, equivalently,

$$\phi'' + 3\phi' - \frac{1}{2}(\phi')^3 + \left(3 - \frac{1}{2}(\phi')^2\right) \frac{V_{,\phi}}{V} = 0, \quad (12)$$

where the primes denote the derivatives with respect to e-folds N .

The standard Hubble-flow parameters are defined by

$$\epsilon_{i+1} = \epsilon'_i / \epsilon_i, \quad \epsilon_0 = H^{-1}. \quad (13)$$

To distinguish the different phases of inflation and compute the one-loop quantum corrections (1LC), we use the first three Hubble-flow parameters,

$$\epsilon \equiv \epsilon_1, \quad \eta \equiv \epsilon_2, \quad \xi \equiv \epsilon_3. \quad (14)$$

The SR phase is characterized by the condition $\epsilon \ll |\eta| \ll 1$, whereas the USR phase is defined by $|\eta| \approx 6$. A transition between SR and USR phases is supposed to be continuous and not instantaneous. For the purpose of evaluating the 1LC, exact values of e-folds at the start and the end of the USR phase are needed. To determine the transition periods, we use the condition proposed in Ref. [25]:

$$|\xi| \geq 1. \quad (15)$$

The results of our numerical calculation are given by Fig. 2.

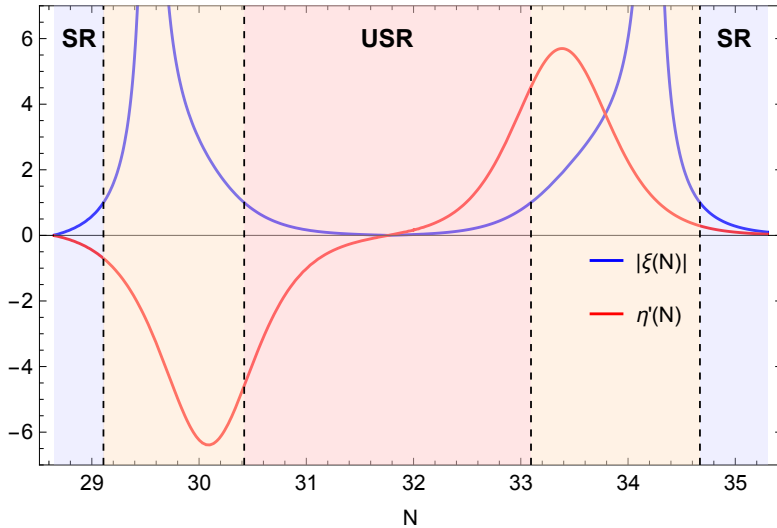


Figure 2: The evolution of η' and $|\xi|$ as the functions of e-folds in the E-model. The vertical dashed lines mark the transitions where $|\xi| = 1$. The parameters of the model are given by set 1 of Table 1 in Section 7.

The start N_s and the end N_e of the USR phase, obtained from the condition $|\xi| = 1$, are directly associated with the SR–USR and USR–SR transitions, respectively. One can also introduce the (transition) sharpness parameter h according to Ref. [26] as

$$h \equiv 6 \frac{\sqrt{\epsilon_V}}{\pi_e}, \quad (16)$$

where $\epsilon_V = V_{,\phi}(\phi_e)/(2V(\phi_e))$ is the standard slow-roll parameter, $\phi_e = \phi(N_e)$, and $\pi_e = \phi'(N_e)$. In the case of a sharp transition, $h \leq -6$, and for a smooth transition $h \rightarrow 0$.

The standard expression for the power spectrum of scalar perturbations in the SR approximation is given by

$$\mathcal{P}_R = \frac{H^2}{8\pi^2\epsilon} , \quad (17)$$

that is the simple tool for analyzing a dependence of the power spectrum on the model parameters. The shape of the power spectrum for some values of the parameter α , obtained by numerical calculations based on (17), is given by Fig. 3.

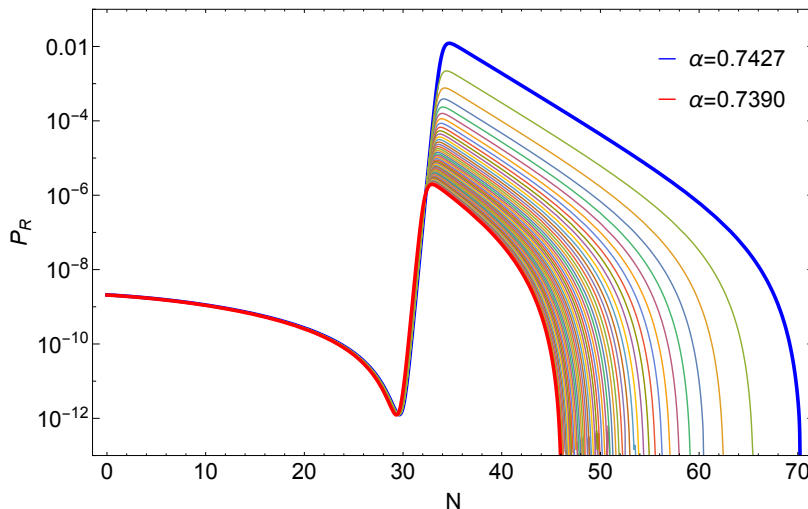


Figure 3: The profiles of the power spectrum of scalar perturbations in the SR approximation in the E-model for $\alpha \in [0.7427, \dots, 0.7390]$ with small and evenly spaced steps. For each value of α , the scalar potential is shifted by an additive constant to get $V(0) = 0$. The other parameters are given by set 1 of Table 1 in Section 7.

As is evident from Fig. 3, the shape of the power spectrum is sensitive to changes in α . When α increases, the peak amplitude of the spectrum also grows. Furthermore, sensitivity of the peak amplitude against changes of α increases with larger values of α . This relation is illustrated in Fig. 4.

A curvature perturbation during inflation, $\zeta_k(N)$, can be expressed in terms of v_k as $\zeta_k \equiv v_k/z$, where $z \equiv a \cdot \phi'$. The variable v_k obeys the Mukhanov-Sasaki (MS) equation

$$v_k'' + (1 - \epsilon) v_k' + \left[\frac{k^2}{a^2 H^2} + (1 + \eta/2)(\epsilon - \eta/2 - 2) - \eta'/2 \right] v_k = 0 . \quad (18)$$

We solve this equation separately for its real and imaginary parts. For each mode, an integration starts five e-folds before the horizon crossing. In terms of the real and imaginary parts of v_k , the initial (Bunch-Davies) conditions are

$$\text{Re}(v_k) = \frac{1}{\sqrt{2k}} , \quad \text{Re}(v_k') = 0 , \quad \text{Im}(v_k) = 0 , \quad \text{Im}(v_k') = -\frac{i}{k_{\text{in}}} \sqrt{\frac{k}{2}} , \quad (19)$$

where k_{in} is the mode that crossed the horizon at the start of integration.

Based on solutions to Eq. (19), the exact scalar power spectrum is computed as

$$\mathcal{P}_\zeta(k) = \frac{k^3}{2\pi^2} \left| \frac{v_k}{z} \right|^2 , \quad (20)$$

where each mode is evaluated at the end of inflation.

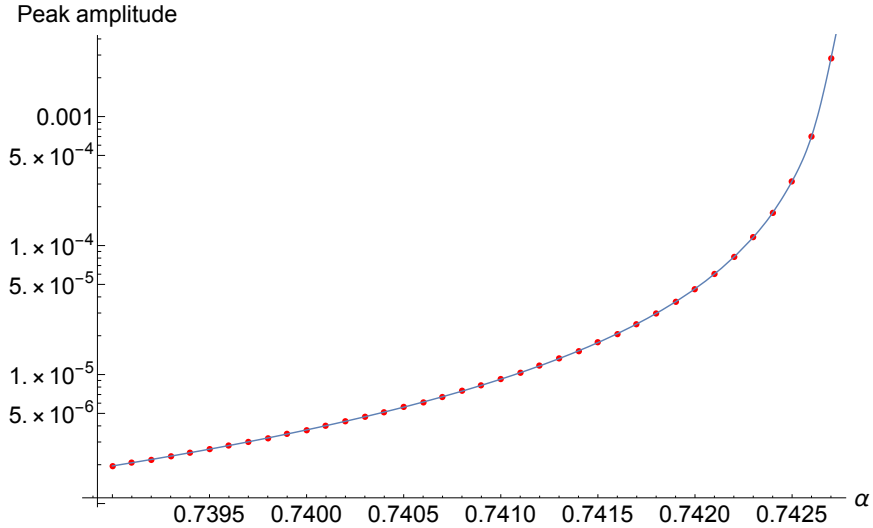


Figure 4: The amplitude of the peak in the power spectrum of scalar perturbations in the SR approximation for the E-model in the logarithmic scale with $\alpha \in [0.7427, \dots, 0.7390]$ in small and evenly spaced steps. The other parameters of the model are given by set 1 of Table 1 in Section 7.

The power spectrum of scalar perturbations can be approximated by the broken power-law fit as

$$\mathcal{P}_{\text{BPL}} = A \frac{\alpha_1 + \beta_1}{\beta_1 (k/k_*)^{-\alpha_1} + \alpha_1 (k/k_*)^{\beta_1}}, \quad (21)$$

where the parameters α_1 and β_1 describe growth and decay of the spectrum around its peak, respectively. The profiles described by Eq. (21) often arise in the single-field inflation models with USR between two SR [27–30]. As is illustrated by Fig. 5 obtained from our numerical calculations, the broken power law fit (21) gives a good approximation for the peak of the power spectrum in the E-model.

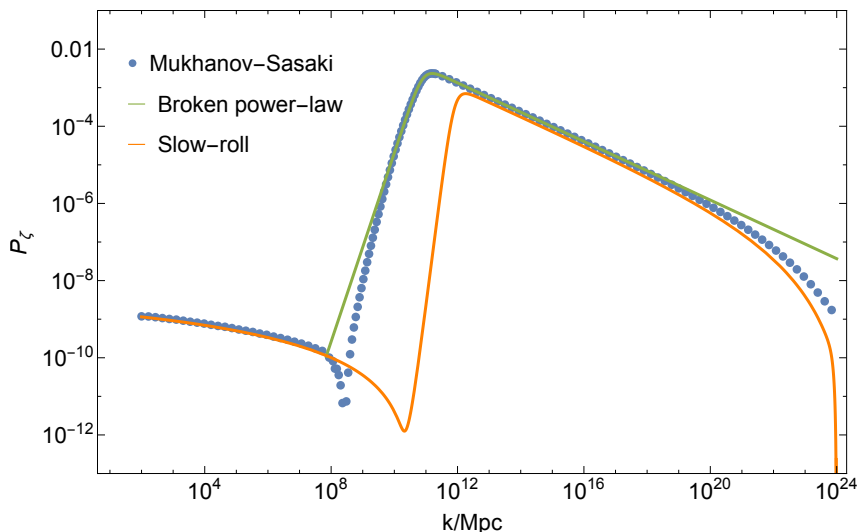


Figure 5: The exact power spectrum of scalar perturbations derived from the MS equation (19) together with the broken power-law (BPL) fit and the slow-roll approximation in the E-model. The BPL fit parameters are $A = 0.00233$, $\alpha_1 = 2.446$, $\beta_1 = 0.379$, and $k_* = 1.57 \cdot 10^{11}$. The parameters of the E-model are given by set 1 of Table 1 in Section 7.

4 One-loop quantum correction in the E-model

For a numerical calculation of the one-loop correction (1LC) to the scalar power spectrum, we adopt Eq. (3.10) from Ref. [25] that takes into account cubic interactions and reads

$$\begin{aligned} \mathcal{P}_\zeta(p; N)_{1\text{L}} = & \frac{p^3}{\pi^4} \int_{N_i}^{N_f} dN_1 \epsilon(N_1) \frac{d\eta(N_1)}{dN_1} (a(N_1))^2 \int_{N_i}^{N_1} dN_2 \epsilon(N_2) \frac{d\eta(N_2)}{dN_2} (a(N_2))^2 \\ & \int_{k_s}^{k_e} dk k^2 \text{Im} \left[\zeta_p(N) a(N_1) H(N_1) a(N_2) H(N_2) \frac{d}{dN_2} \left[\zeta_p^*(N_2) (\zeta_k^*(N_2))^2 \right] \right. \\ & \left. \times \left\{ \zeta_p^I(N) \frac{d}{dN_1} \left[\zeta_p^R(N_1) (\zeta_k(N_1))^2 \right] - \zeta_p^R(N) \frac{d}{dN_1} \left[\zeta_p^I(N_1) (\zeta_k(N_1))^2 \right] \right\} \right], \end{aligned} \quad (22)$$

where the large-scale mode p is supposed to be located in the plateau region, being sufficiently separated from the peak scale k_{peak} . We take $p = k_{\text{peak}}/10^5$ in our E-model. The e-folds N are chosen well after the mode p crosses the horizon $p \ll aH$, when ζ_p approaches a constant value. In (22), ζ_p^R and ζ_p^I denote real and imaginary part of ζ_p , respectively. The integration over the e-folds in (22) is supposed to be performed over the period when η' is large, thus ensuring all relevant contributions to the 1LC are captured. Therefore, the integration bounds are defined from N_i , around an e-fold before the first transition, to N_f , around an e-fold after the last transition. The loop integration over k is supposed to be limited to the USR phase with $k_s = a(N_s)H(N_s)$ and $k_e = a(N_e)H(N_e)$.

A derivation of Eq. (22) in Ref. [25] used the same method as in Ref. [6] but evaluated the loop numerically without assuming instantaneous transitions. Equation (22) is suitable to our purposes because it allows us to compute the 1LC starting from the scalar potential. We used an original code for evaluating Eq. (22) in the E-model.

We define the relative 1LC against the tree-level scalar power spectrum as

$$\delta_{1\text{L}} = \frac{\mathcal{P}_\zeta(p; N)_{1\text{L}}}{\mathcal{P}_\zeta(p)} \cdot 100 \% . \quad (23)$$

It follows from the results of our numerical calculations collected in Table 2 of Sec. 7 that the E-model has mild SR-USR transitions characterized by $|h| < 6$. The 1LC from cubic and quartic interactions was also studied in Ref. [11], where it was shown that the cubic interaction dominates over the quartic one when $|h| < 6$. In particular, according to Eqs. (5.28) and (5.29) in Ref. [11], one has

$$\frac{\delta_{\text{H}_3}}{\delta_{\text{H}_4}} = \frac{108h(h+8)\Delta N_{\text{USR}}}{6(h(h+6)+36)\Delta N_{\text{USR}} - h + 6} . \quad (24)$$

However, the value of δ_{H_3} given in the numerator above differs from our numerical results obtained from Eq. (22). We believe this disagreement is due to the difference between sharp and mild transitions where large one-loop corrections are diminished during the subsequent evolution of curvature perturbations after the USR phase.

In the E-model with the parameter set 1 in Table 1 and Table 2, we find $\delta_{\text{H}_3}/\delta_{\text{H}_4} = -5.9$, so the cubic interaction is dominant indeed.

5 PBH-production-induced gravitational waves

Large scalar perturbations, whose amplitudes exceed the CMB amplitude A_s by six or seven orders of magnitude (see Fig. 5), may lead to a detectable stochastic GW background

because tensor modes are sourced by scalar modes already in the second order with respect to perturbations, see Ref. [31] for a review.

The present GW energy density computed in the second order is given by [32, 33],

$$\frac{\Omega_{\text{GW}}(k)}{\Omega_r} = \frac{c_g}{72} \int_{-\frac{1}{\sqrt{3}}}^{\frac{1}{\sqrt{3}}} d d \int_{\frac{1}{\sqrt{3}}}^{\infty} d s \left[\frac{(s^2 - \frac{1}{3})(d^2 - \frac{1}{3})}{s^2 + d^2} \right]^2 \mathcal{P}_\zeta(kx) \mathcal{P}_\zeta(ky) (I_c^2 + I_s^2), \quad (25)$$

where Ω_r is the present-day radiation density, $h^2\Omega_r \approx 4.2 \cdot 10^{-5}$ according to Ref. [1], normalized by the current Hubble parameter $h = 0.674$ (if Hubble tension is ignored). The coefficient $c_g = 0.4$ is related to the number of the effective degrees of freedom in thermal radiation when assuming the Standard Model physics. The variables x and y are related to the integration variables as $x = \frac{\sqrt{3}}{2}(s + d)$, and $y = \frac{\sqrt{3}}{2}(s - d)$, and the functions I_c and I_s are given by [32, 33],

$$I_s = -36 \frac{s^2 + d^2 - 2}{(s^2 - d^2)^2} \left[\frac{s^2 + d^2 - 2}{s^2 - d^2} \log \left| \frac{d^2 - 1}{s^2 - 1} \right| + 2 \right], \quad (26)$$

$$I_c = -36\pi \frac{(s^2 + d^2 - 2)^2}{(s^2 - d^2)^3} \theta(s - 1),$$

with the Heaviside step function θ . It is worth noticing that the GW density profile obtained from Eq.(25) can be influenced by non-Gaussianity (see Eqs. (16) and (18) in Ref. [34]), so Eq. (25) may acquire a prefactor, $\Omega_{\text{GW}}(k) \rightarrow \mathcal{A}^4 \Omega_{\text{GW}}(k)$. In our analysis, we neglect non-Gaussian effects.

Our results for the induced GW from a numerical calculation of Eq. (25) in the E-model are given in Fig. 6 against the background of the expected sensitivity curves of the future space-based gravitational interferometers LISA [35] and DECIGO [36].

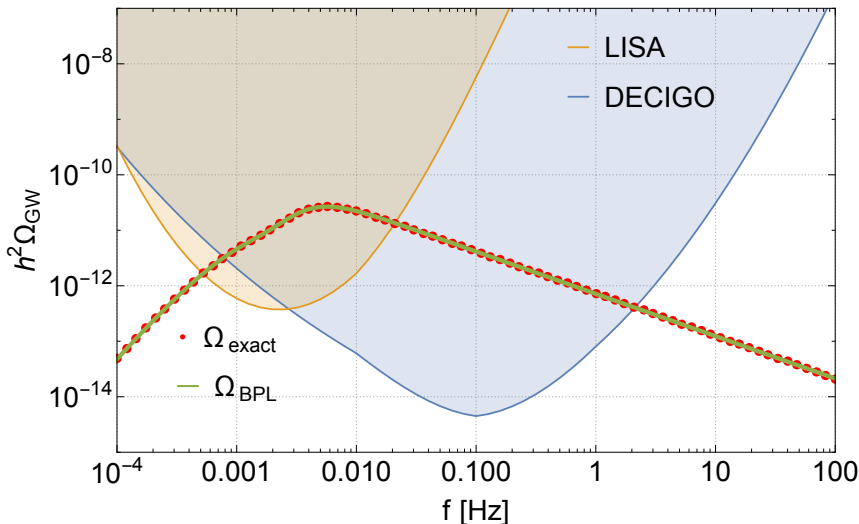
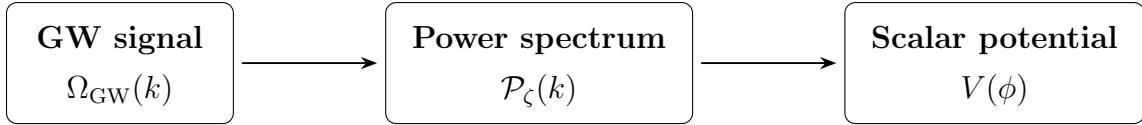


Figure 6: The curve with red dots represents the GW density computed from Eq. (25) by using the scalar perturbation spectrum $\mathcal{P}_\zeta(k)$ obtained from solving the MS equation (19) with the model parameters of set 3 in Table 1 (see Sec. 7). The green line corresponds to the GW density derived by using the broken power-law approximation for the power spectrum. The orange and blue lines show the sensitivity curves of LISA and DECIGO, respectively. The frequency of GW is related to the comoving wavenumber k as $k \simeq 6.47 \cdot 10^{14} (f/\text{Hz}) \text{ Mpc}^{-1}$.

6 Reconstruction of scalar potential from GW signal

When assuming the source of a GW signal due to gravitational collapse of large scalar perturbations after inflation, it is natural to attempt a reconstruction of the (single-field) inflation model underlying this signal. The reconstruction implies the following chain:



This procedure is inevitably ambiguous, and the reconstruction is still a longstanding challenge. For instance, the reconstruction formula proposed by Hodges and Blumenthal in Ref. [37],

$$\frac{1}{V(N)} = -\frac{1}{12\pi^2 M_{\text{pl}}^4} \int \frac{dN}{\mathcal{P}_\zeta(N)}, \quad (27)$$

requires knowledge of the full power spectrum across various scales.

Different power spectra can yield almost identical GW energy density profiles over a limited range of scales, see, e.g., Fig. 1 and Fig. 2 in Ref. [38]. Nevertheless, it is possible to systematically identify the power spectra corresponding to a specific GW energy density curve [30]. Those spectra are often approximated by the broken power law or the log-normal distribution.

The observed CMB window to inflation is limited or small, revealing only the SR plateau at large scales. However, at smaller scales, future GW observations can shed light on the structure of the scalar potential by reconstructing the peak in the power spectrum. Once the peak is identified, the Hubble-flow parameters in its vicinity can be determined. For instance, the parameters α_1 and β_1 in a broken power-law approximation are directly linked to the second slow-roll parameter η [5]. Using these parameters, the scalar potential at smaller scales can be reconstructed by using the relations [28, 39]

$$V(N) = V(N_{\text{ref}}) \exp \left\{ -2 \int_{N_{\text{ref}}}^N dN' \left[\frac{\epsilon(3-\eta)}{3-\epsilon} \right] \right\}, \quad (28)$$

$$\phi(N) = \phi(N_{\text{ref}}) \pm \int_{N_{\text{ref}}}^N dN' \sqrt{2\epsilon}.$$

However, the potential $V(\phi)$ still has to be determined as a function of ϕ over all scales.

We propose to upgrade the reconstruction chain by incorporating theoretically well-motivated models of inflation. This approach focuses on a reconstruction of the parameters of the inflaton potential that are consistent with the reconstructed power spectrum. By doing so, it is possible to identify consistent theoretical models that can explain a given GW signal, while obeying phenomenological constraints across all scales. This process can be performed numerically.

To illustrate this approach, let us consider the reconstructed power spectrum $\mathcal{P}_\zeta^{\text{rec}}(k)$ derived from a hypothetical GW signal. The goal is to determine the set of parameters $\vec{\theta}$ in a scalar potential $V(\phi, \vec{\theta})$ that generates the power spectrum $\mathcal{P}_\zeta(k, \vec{\theta})$ fitting the reconstructed one, $\mathcal{P}_\zeta(k, \vec{\theta}) \approx \mathcal{P}_\zeta^{\text{rec}}(k)$. This task can be formalized as the minimization problem for the functional

$$S(\vec{\theta}) = \sum_i \left[\mathcal{P}_\zeta(k_i; \vec{\theta}) - \mathcal{P}_\zeta^{\text{rec}}(k_i) \right]^2, \quad (29)$$

and then solved by using the Levenberg-Marquardt algorithm. This method requires an initial guess for $\vec{\theta}$ that can be obtained numerically.

First, we find the function $\phi_{\text{sol}}[N, \vec{\theta}]$ as a numerical solution to the equation of motion (12) with a given set $\vec{\theta}$. Based on this solution, the power spectrum can be calculated in the form (17). This allows us to manually adjust $\vec{\theta}$ matching the power spectrum in the SR approximation with $\mathcal{P}_{\zeta}^{\text{rec}}(k)$. Fine-tuning at this stage is not necessary, while it suffices to find $\vec{\theta}$ producing a peak in the power spectrum within the range of two or three orders of magnitude in k around the peak of $\mathcal{P}_{\zeta}^{\text{rec}}(k)$. The initial guess for $\vec{\theta}$ can also be guided by analyzing the potential reconstructed from (28).

After that, we numerically construct the function $v[k, \vec{\theta}]$ providing a solution to Eq. (18). Using this solution, we derive $\mathcal{P}_{\zeta}[k_i; \vec{\theta}]$ as in Eq. (20) for a specific range of k , and employ parallel computations. Next, we identify the set of parameters $\vec{\theta}$ in the chosen model whose power spectrum matches $\mathcal{P}_{\zeta}^{\text{rec}}(k)$.

In the case of the E-model under consideration, the procedure described above allowed us to get the parameter Set 3 in Table 1 (see Sec. 7), starting from Ω_{BPL} shown in Fig. 6.

Knowing the inflationary model underlying a given GW signal, allows us to verify whether this model is capable of reproducing the observed signal without conflicting with CMB measurements or quantum corrections. Such verification requires knowledge of the power spectrum beyond the scales directly reconstructed from the GW signal.

7 The results

In this Section, we present our main findings.

Three sets of fine-tuned parameters in our E-model, required for efficient PBH production relevant to DM and GW, are collected in Table 1.

E-Model	Set 1	Set 2	Set 3
α	0.7425	0.74	0.77218
ϕ_i	-0.611325	-0.6112	-0.6415
σ	0.012137	0.0131	0.0125
θ	$-7.29 \cdot 10^{-7}$	$-9.17 \cdot 10^{-7}$	$-7.37 \cdot 10^{-7}$
$(M/M_{\text{Pl}})^2$	$6.3 \cdot 10^{-10}$	$7.2 \cdot 10^{-10}$	$6.3 \cdot 10^{-10}$

Table 1: The fine-tuned parameters for the E-model of inflation and PBH DM.

With those parameters, the E-model satisfies the CMB constraints and allows a production of PBH in the asteroid-mass (atomic size) window, where those PBH may account for a significant part (or the whole) of DM.² Gravitational collapse of scalar perturbations leading to the PBH formation induces the stochastic GW that may be detectable by the future space-based gravitational interferometers such as LISA [35], TAIJI [41], TianQin [42] and DECIGO [36], see Refs. [33, 43, 44] for more about them.

We used the linear approximation for computing the CMB tilt n_s of scalar perturbations and the CMB tensor-to-scalar ratio r from the Hubble-flow parameters at the pivot CMB scale $k_* = 0.05 \text{ Mpc}^{-1}$ at the horizon crossing,

$$n_s = 1 - 2\epsilon - \eta, \quad r = 16\epsilon. \quad (30)$$

²The PBH abundances vary, being dependent on the approach used, see Ref. [40] for a review.

In the E-Model, it leads to approximately 60 e-folds. The current measurements of the CMB give [1]:³

$$n_s = 0.9649 \pm 0.0042 \quad (68\% \text{ C.L.}) , \quad \text{and} \quad r < 0.032 \quad (95\% \text{ C.L.}) . \quad (31)$$

The PBH masses can be estimated as [45, 46]

$$M_{\text{PBH}}(k) \simeq 10^{20} \left(\frac{7 \cdot 10^{12}}{k \cdot \text{Mpc}} \right)^2 \text{ g} . \quad (32)$$

The key observables and the relative values of the one-loop correction (1LC) are given in Table 2.

E-Model	n_s	r	h	ΔN_{USR}	M_{PBH} , g	$\mathcal{P}_\zeta(k_{\text{peak}})$	δ_{1L} , %
Set 1	0.9649	0.01466	-1.472	2.674	$2.2 \cdot 10^{21}$	10^{-3}	1.31
Set 2	0.9649	0.01685	-1.435	2.838	$7.1 \cdot 10^{22}$	$0.5 \cdot 10^{-2}$	2.96
Set 3	0.9649	0.014323	-1.471	2.687	$4.6 \cdot 10^{18}$	10^{-3}	1.33

Table 2: The CMB tilts n_s and r , the sharpness parameter h , the USR phase duration ΔN_{USR} , the PBH masses M_{PBH} , the peak amplitude $\mathcal{P}_\zeta(k_{\text{peak}})$, and the relative (against the tree level contribution) one-loop correction δ_{1L} for the parameter sets in Table 1.

We also evaluated the μ -type distortion [47, 48] of the CMB in our model, which places the additional constraints on the primordial power spectrum at smaller scales up to $k \sim 10^4 \text{ Mpc}^{-1}$. The μ -distortion can be estimated by the integral [49–53]

$$\mu \approx \int_{k_{\text{min}}}^{\infty} \frac{dk}{k} \mathcal{P}_\zeta(k) W_\mu(k) , \quad (33)$$

where the analytic window function $W_\mu(k)$ is given by [52]

$$W_\mu(k) \approx 2.27 \left\{ \exp \left[- \left(\frac{k}{1360} \right)^2 \left(1 + \left(\frac{k}{260} \right)^{0.3} + \frac{k}{340} \right)^{-1} \right] - \exp \left[- \left(\frac{k}{32} \right)^2 \right] \right\} , \quad (34)$$

and $k_{\text{min}} \simeq 1 \text{ Mpc}^{-1}$. The current upper bound from COBE/FIRAS observations [54] is given by $\mu < 9 \cdot 10^{-5}$ (95% C.L.). In our model, for each parameter set in Table 1, we find $\mu \simeq 10^{-10}$ that is significantly below the observational limit.

The results of our numerical calculations, related to the data in Table 1 and Table 2, are given in Figs. 1–6. In particular, we found the one-loop correction (1LC) in our E-model does not exceed a few percent, being primarily depending upon the amplitude of the peak in the scalar power spectrum. These results are consistent with the conclusions in Ref. [25].

We also found that extending the limits of integration in Eq. (22) has a negligible effect on the results, thus confirming the dominant contribution to the 1LC comes from the cubic interaction during the period when η' is large. An impact of the quartic interaction deserves future research.

The inverse reconstruction of the parameters in the E-model from the GW spectrum demonstrates its significance as the reasonable framework for interpreting future GW measurements.

³The running of the scalar spectral index n_s , usually denoted by α_s , is also an observable. Its observational bounds are satisfied for each set of the parameters in Table 1.

8 Conclusion

We conclude with a few comments.

The E-model defined by Eq. (7) is a deformation of the Starobinsky model of inflation [20] on smaller scales. Like any other viable single-large-field model of inflation, it is tightly constrained but is not ruled out by CMB measurements of (A_s, n_s, r) and the Swampland conjectures [55]. The E-type α -attractor model investigated in this paper is different from the T-type α -attractor models and the other single-field models of inflation and PBH production studied in the literature [5, 56, 57].

The 1LC to the power spectrum of our E-model was found to be merely a few percent against the tree-level contribution, which further supports the validity of the model. The estimates of the two-loop contribution (2LC) in the literature [14, 17] suggest the 2LC to be roughly the 1LC squared, which is negligible in our E-model also.

Reheating (particle production after inflation) in our E-model is the same as that in the Starobinsky model, which was well studied in the literature, see e.g., Ref. [58] and references therein, so we do not expect tensions with standard cosmology [59].

Simple single-field SR models of inflation were motivated by the almost scale-invariant CMB spectrum and approximately Gaussian fluctuations. Though being tightly constrained, those models have high predictive power, and they may be either confirmed or falsified by future cosmological measurements. Non-Gaussianities (or non-linear effects) at peak scales are expected to be of the local type with the small amplitude of $f_{\text{NL}} \sim \mathcal{O}(0.1)$ [60], even though this key estimate may be not enough to claim the validity of the perturbative approach. Non-perturbative non-Gaussianities [61] are also expected due to stochastic effects during inflation but their inclusion is beyond the scope of this paper.

We avoided presenting our results about a specific PBH fraction in DM, based on our E-model, because the PBH abundance is highly sensitive to the peak in the power spectrum, while the standard (Press-Schechter) formalism for its evaluation does not produce reliable results.

Acknowledgements

DF and SVK were partially supported by Tomsk State University under the development program Priority-2030. DF was supported by the BASIS Foundation for Advancement of Theoretical Physics and Mathematics. SVK was also supported by Tokyo Metropolitan University, the Japanese Society for Promotion of Science under the grant No. 22K03624, and the World Premier International Research Center Initiative, MEXT, Japan.

References

- [1] **Planck** Collaboration, Y. Akrami *et al.*, “Planck 2018 results. X. Constraints on inflation,” *Astron. Astrophys.* **641** (2020) A10, [arXiv:1807.06211 \[astro-ph.CO\]](#).
- [2] M. van Beest, J. Calderón-Infante, D. Mirfendereski, and I. Valenzuela, “Lectures on the Swampland Program in String Compactifications,” *Phys. Rept.* **989** (2022) 1–50, [arXiv:2102.01111 \[hep-th\]](#).
- [3] I. D. Novikov and Y. B. Zeldovic, “Cosmology,” *Ann. Rev. Astron. Astrophys.* **5** (1967) 627–649.
- [4] S. Hawking, “Gravitationally collapsed objects of very low mass,” *Mon. Not. Roy. Astron. Soc.* **152** (1971) 75.

- [5] A. Karam, N. Koivunen, E. Tomberg, V. Vaskonen, and H. Veermäe, “Anatomy of single-field inflationary models for primordial black holes,” *JCAP* **03** (2023) 013, [arXiv:2205.13540 \[astro-ph.CO\]](#).
- [6] J. Kristiano and J. Yokoyama, “Constraining Primordial Black Hole Formation from Single-Field Inflation,” *Phys. Rev. Lett.* **132** no. 22, (2024) 221003, [arXiv:2211.03395 \[hep-th\]](#).
- [7] A. Riotto, “The Primordial Black Hole Formation from Single-Field Inflation is Not Ruled Out,” [arXiv:2301.00599 \[astro-ph.CO\]](#).
- [8] J. Kristiano and J. Yokoyama, “Note on the bispectrum and one-loop corrections in single-field inflation with primordial black hole formation,” *Phys. Rev. D* **109** no. 10, (2024) 103541, [arXiv:2303.00341 \[hep-th\]](#).
- [9] A. Riotto, “The Primordial Black Hole Formation from Single-Field Inflation is Still Not Ruled Out,” [arXiv:2303.01727 \[astro-ph.CO\]](#).
- [10] S. Choudhury, M. R. Gangopadhyay, and M. Sami, “No-go for the formation of heavy mass Primordial Black Holes in Single Field Inflation,” *Eur. Phys. J. C* **84** no. 9, (2024) 884, [arXiv:2301.10000 \[astro-ph.CO\]](#).
- [11] H. Firouzjahi, “One-loop corrections in power spectrum in single field inflation,” *JCAP* **10** (2023) 006, [arXiv:2303.12025 \[astro-ph.CO\]](#).
- [12] H. Motohashi and Y. Tada, “Squeezed bispectrum and one-loop corrections in transient constant-roll inflation,” *JCAP* **08** (2023) 069, [arXiv:2303.16035 \[astro-ph.CO\]](#).
- [13] H. Firouzjahi and A. Riotto, “Primordial Black Holes and loops in single-field inflation,” *JCAP* **02** (2024) 021, [arXiv:2304.07801 \[astro-ph.CO\]](#).
- [14] S. Saburov and S. V. Ketov, “Quantum Loop Corrections in the Modified Gravity Model of Starobinsky Inflation with Primordial Black Hole Production,” *Universe* **10** no. 9, (2024) 354, [arXiv:2402.02934 \[gr-qc\]](#).
- [15] K. Inomata, “Superhorizon Curvature Perturbations Are Protected against One-Loop Corrections,” *Phys. Rev. Lett.* **133** no. 14, (2024) 141001, [arXiv:2403.04682 \[astro-ph.CO\]](#).
- [16] J. Kristiano and J. Yokoyama, “Comparing sharp and smooth transitions of the second slow-roll parameter in single-field inflation,” *JCAP* **10** (2024) 036, [arXiv:2405.12145 \[astro-ph.CO\]](#).
- [17] H. Firouzjahi, “Two-loop corrections in power spectrum in models of inflation with PBHs formation,” [arXiv:2411.10253 \[hep-ph\]](#).
- [18] R. Kallosh and A. Linde, “Universality Class in Conformal Inflation,” *JCAP* **07** (2013) 002, [arXiv:1306.5220 \[hep-th\]](#).
- [19] M. Galante, R. Kallosh, A. Linde, and D. Roest, “Unity of Cosmological Inflation Attractors,” *Phys. Rev. Lett.* **114** no. 14, (2015) 141302, [arXiv:1412.3797 \[hep-th\]](#).
- [20] A. A. Starobinsky, “A New Type of Isotropic Cosmological Models Without Singularity,” *Phys. Lett. B* **91** (1980) 99–102.

- [21] S. V. Ketov, “On the equivalence of Starobinsky and Higgs inflationary models in gravity and supergravity,” *J. Phys. A* **53** no. 8, (2020) 084001, [arXiv:1911.01008 \[hep-th\]](#).
- [22] I. Dalianis, A. Kehagias, and G. Tringas, “Primordial black holes from α -attractors,” *JCAP* **01** (2019) 037, [arXiv:1805.09483 \[astro-ph.CO\]](#).
- [23] D. Frolovsky, S. V. Ketov, and S. Saburov, “E-models of inflation and primordial black holes,” *Front. in Phys.* **10** (2022) 1005333, [arXiv:2207.11878 \[astro-ph.CO\]](#).
- [24] D. Frolovsky and S. V. Ketov, “Production of Primordial Black Holes in Improved E-Models of Inflation,” *Universe* **9** no. 6, (2023) 294, [arXiv:2304.12558 \[astro-ph.CO\]](#).
- [25] M. W. Davies, L. Iacconi, and D. J. Mulryne, “Numerical 1-loop correction from a potential yielding ultra-slow-roll dynamics,” *JCAP* **04** (2024) 050, [arXiv:2312.05694 \[astro-ph.CO\]](#).
- [26] Y.-F. Cai, X. Chen, M. H. Namjoo, M. Sasaki, D.-G. Wang, and Z. Wang, “Revisiting non-Gaussianity from non-attractor inflation models,” *JCAP* **05** (2018) 012, [arXiv:1712.09998 \[astro-ph.CO\]](#).
- [27] V. Vaskonen and H. Veermäe, “Did NANOGrav see a signal from primordial black hole formation?,” *Phys. Rev. Lett.* **126** no. 5, (2021) 051303, [arXiv:2009.07832 \[astro-ph.CO\]](#).
- [28] C. T. Byrnes, P. S. Cole, and S. P. Patil, “Steepest growth of the power spectrum and primordial black holes,” *JCAP* **06** (2019) 028, [arXiv:1811.11158 \[astro-ph.CO\]](#).
- [29] P. Carrilho, K. A. Malik, and D. J. Mulryne, “Dissecting the growth of the power spectrum for primordial black holes,” *Phys. Rev. D* **100** no. 10, (2019) 103529, [arXiv:1907.05237 \[astro-ph.CO\]](#).
- [30] **LISA Cosmology Working Group** Collaboration, M. Braglia *et al.*, “Gravitational waves from inflation in LISA: reconstruction pipeline and physics interpretation,” *JCAP* **11** (2024) 032, [arXiv:2407.04356 \[astro-ph.CO\]](#).
- [31] G. Domènech, “Scalar Induced Gravitational Waves Review,” *Universe* **7** no. 11, (2021) 398, [arXiv:2109.01398 \[gr-qc\]](#).
- [32] J. R. Espinosa, D. Racco, and A. Riotto, “A Cosmological Signature of the SM Higgs Instability: Gravitational Waves,” *JCAP* **09** (2018) 012, [arXiv:1804.07732 \[hep-ph\]](#).
- [33] N. Bartolo, V. De Luca, G. Franciolini, A. Lewis, M. Peloso, and A. Riotto, “Primordial Black Hole Dark Matter: LISA Serendipity,” *Phys. Rev. Lett.* **122** no. 21, (2019) 211301, [arXiv:1810.12218 \[astro-ph.CO\]](#).
- [34] A. J. Iovino, S. Matarrese, G. Perna, A. Ricciardone, and A. Riotto, “How Well Do We Know the Scalar-Induced Gravitational Waves?,” [arXiv:2412.06764 \[astro-ph.CO\]](#).
- [35] **LISA** Collaboration, P. Amaro-Seoane *et al.*, “Laser Interferometer Space Antenna,” [arXiv:1702.00786 \[astro-ph.IM\]](#).

- [36] H. Kudoh, A. Taruya, T. Hiramatsu, and Y. Himemoto, “Detecting a gravitational-wave background with next-generation space interferometers,” *Phys. Rev. D* **73** (2006) 064006, [arXiv:gr-qc/0511145](#).
- [37] H. M. Hodges and G. R. Blumenthal, “Arbitrariness of inflationary fluctuation spectra,” *Phys. Rev. D* **42** (1990) 3329–3333.
- [38] D. Frolovsky, F. Kuhnel, and I. Stamou, “Reconstructing Primordial Black Hole Power Spectra from Gravitational Waves,” [arXiv:2404.06547 \[astro-ph.CO\]](#).
- [39] G. Franciolini and A. Urbano, “Primordial black hole dark matter from inflation: The reverse engineering approach,” *Phys. Rev. D* **106** no. 12, (2022) 123519, [arXiv:2207.10056 \[astro-ph.CO\]](#).
- [40] S. Pi, M. Sasaki, V. Takhistov, and J. Wang, “Primordial Black Hole Formation from Power Spectrum with Finite-width,” [arXiv:2501.00295 \[astro-ph.CO\]](#).
- [41] X. Gong *et al.*, “Descope of the ALIA mission,” *J. Phys. Conf. Ser.* **610** no. 1, (2015) 012011, [arXiv:1410.7296 \[gr-qc\]](#).
- [42] **TianQin** Collaboration, J. Luo *et al.*, “TianQin: a space-borne gravitational wave detector,” *Class. Quant. Grav.* **33** no. 3, (2016) 035010, [arXiv:1512.02076 \[astro-ph.IM\]](#).
- [43] J. Garcia-Bellido, M. Peloso, and C. Unal, “Gravitational Wave signatures of inflationary models from Primordial Black Hole Dark Matter,” *JCAP* **09** (2017) 013, [arXiv:1707.02441 \[astro-ph.CO\]](#).
- [44] R.-g. Cai, S. Pi, and M. Sasaki, “Gravitational Waves Induced by non-Gaussian Scalar Perturbations,” *Phys. Rev. Lett.* **122** no. 20, (2019) 201101, [arXiv:1810.11000 \[astro-ph.CO\]](#).
- [45] K. Inomata, M. Kawasaki, K. Mukaida, Y. Tada, and T. T. Yanagida, “Inflationary Primordial Black Holes as All Dark Matter,” *Phys. Rev. D* **96** no. 4, (2017) 043504, [arXiv:1701.02544 \[astro-ph.CO\]](#).
- [46] K. Inomata, M. Kawasaki, K. Mukaida, and T. T. Yanagida, “Double inflation as a single origin of primordial black holes for all dark matter and LIGO observations,” *Phys. Rev. D* **97** no. 4, (2018) 043514, [arXiv:1711.06129 \[astro-ph.CO\]](#).
- [47] Y. B. Zeldovich and R. A. Sunyaev, “The Interaction of Matter and Radiation in a Hot-Model Universe,” *Astrophys. Space Sci.* **4** (1969) 301–316.
- [48] J. Chluba and R. A. Sunyaev, “The evolution of CMB spectral distortions in the early Universe,” *Mon. Not. Roy. Astron. Soc.* **419** (2012) 1294–1314, [arXiv:1109.6552 \[astro-ph.CO\]](#).
- [49] J. Chluba, J. Hamann, and S. P. Patil, “Features and New Physical Scales in Primordial Observables: Theory and Observation,” *Int. J. Mod. Phys. D* **24** no. 10, (2015) 1530023, [arXiv:1505.01834 \[astro-ph.CO\]](#).
- [50] N. Schöneberg, M. Lucca, and D. C. Hooper, “Constraining the inflationary potential with spectral distortions,” *JCAP* **03** (2021) 036, [arXiv:2010.07814 \[astro-ph.CO\]](#).
- [51] C. Ünal, E. D. Kovetz, and S. P. Patil, “Multimessenger probes of inflationary fluctuations and primordial black holes,” *Phys. Rev. D* **103** no. 6, (2021) 063519, [arXiv:2008.11184 \[astro-ph.CO\]](#).

- [52] E. Pajer and M. Zaldarriaga, “A New Window on Primordial non-Gaussianity,” *Phys. Rev. Lett.* **109** (2012) 021302, [arXiv:1201.5375](#) [[astro-ph.CO](#)].
- [53] M. Tagliacuci, M. Braglia, F. Finelli, and M. Pieroni, “Quest for CMB spectral distortions to probe the scalar-induced gravitational wave background interpretation of pulsar timing array data,” *Phys. Rev. D* **111** no. 2, (2025) L021305, [arXiv:2310.08527](#) [[astro-ph.CO](#)].
- [54] D. J. Fixsen, E. S. Cheng, J. M. Gales, J. C. Mather, R. A. Shafer, and E. L. Wright, “The Cosmic Microwave Background spectrum from the full COBE FIRAS data set,” *Astrophys. J.* **473** (1996) 576, [arXiv:astro-ph/9605054](#).
- [55] M. Scalisi and I. Valenzuela, “Swampland distance conjecture, inflation and α -attractors,” *JHEP* **08** (2019) 160, [arXiv:1812.07558](#) [[hep-th](#)].
- [56] J. Martin, C. Ringeval, and V. Vennin, “Encyclopædia Inflationaris: Oviparous Edition,” *Phys. Dark Univ.* **5-6** (2014) 75–235, [arXiv:1303.3787](#) [[astro-ph.CO](#)].
- [57] J. Martin, C. Ringeval, and V. Vennin, “Cosmic Inflation at the crossroads,” *JCAP* **07** (2024) 087, [arXiv:2404.10647](#) [[astro-ph.CO](#)].
- [58] H. Jeong, K. Kamada, A. A. Starobinsky, and J. Yokoyama, “Reheating process in the R^2 inflationary model with the baryogenesis scenario,” *JCAP* **11** (2023) 023, [arXiv:2305.14273](#) [[hep-ph](#)].
- [59] S. Allegrini, L. Del Grosso, A. J. Iovino, and A. Urbano, “Is the formation of primordial black holes from single-field inflation compatible with standard cosmology?,” [arXiv:2412.14049](#) [[astro-ph.CO](#)].
- [60] L. Iacconi, M. Bacchi, L. F. Guimarães, and F. T. Falciano, “Testing inflation on all scales: a case study with α -attractors,” [arXiv:2412.02544](#) [[astro-ph.CO](#)].
- [61] V. Vennin and D. Wands, “Quantum diffusion and large primordial perturbations from inflation,” [arXiv:2402.12672](#) [[astro-ph.CO](#)].